Available online at www.sciencedirect.com
SCIENCE DIRECT
Medical Engineering & Physics 27 (2005) 884–892
Medical Engineering & Physics
www.elsevier.com/locate/medengphy

Non-linear elastic properties of the lingual and facial tissues assessed by indentation technique Application to the biomechanics of speech production

J.M. Gerard [a,b], J. Ohayon [a], V. Luboz [a], P. Perrier [b], Y. Payan [a,*]

[a] *Laboratoire TIMC/IMAG, Faculte de Medecine de Grenoble, Institut d'Ingenierie de l'Information de Sante, Pavillon Taillefer, UMR CNRS 5525, Université Joseph Fourier de Grenoble, 38706 La Tronche, France*
[b] *Institut de la Communication Parlée, CNRS, INP Grenoble, France*

Received 22 October 2004; received in revised form 9 August 2005; accepted 30 August 2005

Abstract

This paper aims at characterizing the mechanical behavior of two human anatomical structures, namely the tongue and the cheek. For this, an indentation experiment was provided, by measuring the mechanical response of tongue and cheek tissues removed from the fresh cadaver of a 74 year old woman. Non-linear relationships were observed between the force applied to the tissues and the corresponding displacements. To infer the mechanical constitutive laws from these measurements, a finite element (FE) analysis was provided. This analysis aimed at simulating the indentation experiment. An optimization process was used to determine the FE constitutive laws that provided the non-linear force/displacements observed during the indentation experiments. The tongue constitutive law was used for simulations provided by a 3D FE biomechanical model of the human tongue. This dynamical model was designed to study speech production. Given a set of tongue muscular commands, which levels correspond to the force classically measured during speech production, the FE model successfully simulated the main tongue movements observed during speech data.

Keywords: Soft tissues; Constitutive law; Indentation; Finite element method; Hyperelasticity; Tongue; Cheeks

1. Introduction

The movements of the speech articulators, the jaw, the tongue, the velum, the lips and the vocal folds, together with the air-flow propagation from the lungs to the lips, are the physical basis of speech production. Their time and amplitude characteristics determine the temporal variation of the acoustical and visual signals of speech, which are in turn the physical stimuli that will be used by the listeners to perceive and understand speech. Consequently, to study and model, from a cognitive point of view, the speech communication process, and especially the interaction between production and perception, it is essential to clarify the following questions:

(1) To which extent do the physical properties of the speech articulators constrain the articulatory trajectories over time and, then, the time variation of the acoustic and visual signals? [1,2]
(2) How can the central nervous system impose speech specific properties to the articulatory movements in order to convey the linguistic information that is the essence of speech communication? [3]
(3) Do the auditory and visual human perception systems use knowledge about the physical properties of the speech apparatus to analyse and interpret the articulatory and acoustic speech signals? [4,5].

In addition, just like the car driver who needs to have some ideas about the way his car behaves on the road, in order to control it, it is necessary for the speakers to have some representations of the way their speech articulators respond to

* Corresponding author. Tel.: +33 456 520001; fax: +33 456 520055.
E-mail address: Yohan.Payan@imag.fr (Y. Payan).

1350-4533/$ – see front matter © 2005 IPEM. Published by Elsevier Ltd. All rights reserved.
doi:10.1016/j.medengphy.2005.08.001

motor commands, in order to produce intelligible speech. Therefore, to understand speech motor control, a key issue concerns the complexity of these representations in the speakers' mind. To address this issue, it is necessary for us, first, to characterize which are the physical properties of the speech articulators, and, second, to test to which extent simplified representations of these properties are compatible with the time and position accuracy requirements of speech communication [6–8].

For all these reasons, our research group has been working for the last 10 years on the design of a biomechanical model of the speech production apparatus and on models of speech motor control [1,9,10]. As concerns biomechanical modeling, the main efforts have been firstly devoted to the tongue [1,10] that is the most important and the most complex articulator of the vocal tract, and secondly to the face [11]. The study presented in this paper contributes to this general project as it aims at characterizing as realistically as possible the elasticity properties of the tongue and the cheeks. Since we aim at testing speech motor control models by driving biomechanical models and by comparing simulations with data collected on human speakers [12], such an elastic characterization is a major challenge, to ensure the reliability of our approach.

2. Biomechanical modeling of the biological soft tissues: a continuum approach

From continuum mechanics perspective, stress, strain and displacement fields of human soft tissues are piecewise continuous functions of space coordinates and time. The partial differential equations (PDE) that governs continuum mechanics are numerically solved over a piecewise discretization of the domain, usually by means of the finite element method [13]. Two modeling assumptions are usually made, which make the numerical resolution more or less complex and time consuming. The first assumption concerns the maximal level of strain that can be observed inside the body. If this level is less than 10% (i.e. if for any elementary vector inside the body its length does not vary by a factor that is superior to 0.1), the "small strain" hypothesis can be made, which assumes a linear geometrical resolution of PDE. Otherwise, a "large strain" framework is necessary, which means a much more complex resolution of the numerical system. The second assumption concerns the so-called "rheology" of the body, i.e. the "mechanical" relation between strain and stress (the term "constitutive law" is also used). If this relation can be assumed to be linear, an elasticity tensor is computed to link the stress and strain tensors. On the contrary, if a linear law does not account properly for the mechanical behavior of the tissues, a non-linear law can be chosen to account for the hyperelastic behavior of soft tissues (see [13] for more details).

In the case of lingual tissues, the measurements provided by Napadow et al. [14] definitively discard the "small strain" hypothesis since tissue elongation as large as 200% (respectively 160% for tongue contraction) were reported. Therefore, a large strain framework seems necessary for an accurate modeling of tongue tissues. Concerning facial tissues, such a large strain-modeling framework does not seem so clearly necessary. Indeed, no measurement was provided in the literature for facial tissues elongation and/or contraction during speech production.

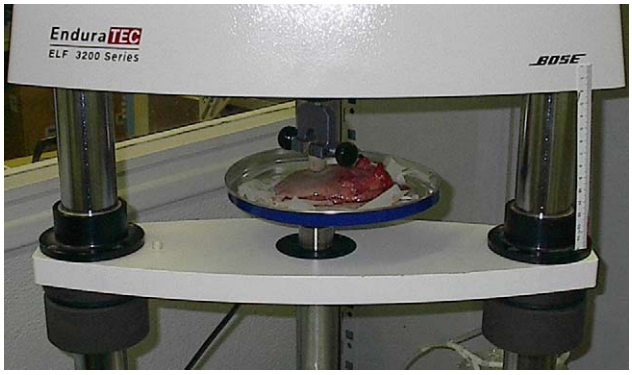

Fig. 1. Indentation device with human tongue being indented in the middle.

The choice between a linear and a non-linear constitutive law for tongue and/or face tissues, is much more delicate. Over the past decade, several experimental and theoretical joined studies have been made, in order to characterize the mechanical behavior of ex vivo tissue samples such as skin [15,16], brain [17], liver [18], kidney [19], or heart [20]. Unfortunately, to our knowledge, no experimental data were provided concerning the mechanical behavior of the tongue or the face.

For this reason, a set of indentation experiments has been carried out on a tongue and a cheeks piece collected on a fresh human cadaver. This experimental work is going to be presented in the next section. A non-linear constitutive law has been derived from those experiments and the procedure that we set up in this aim will be explained in Section 4. The last section introduces the 3D dynamical finite element model of the human tongue that is used to study speech motor control, assuming a large strain framework and integrating the realistic non-linear constitutive law described in Section 4.

3. Indentation experiment

An indentation experiment aims at estimating the constitutive law of a material. The method consists in exerting a calibrated pressure onto the material and simultaneously recording the corresponding deformations. Measurements provided here have been achieved by using an indentation device from the Enduratec^{TM} Company (Fig. 1). This device, which will be referred later in the paper as Enduratec, is built to characterize the properties of a material with low rigidity and a size on the order of a few centimeters. It is controlled via electro-magnetic actuators and sensors. These actuators can drive a thin plate of metal or jaws for the load

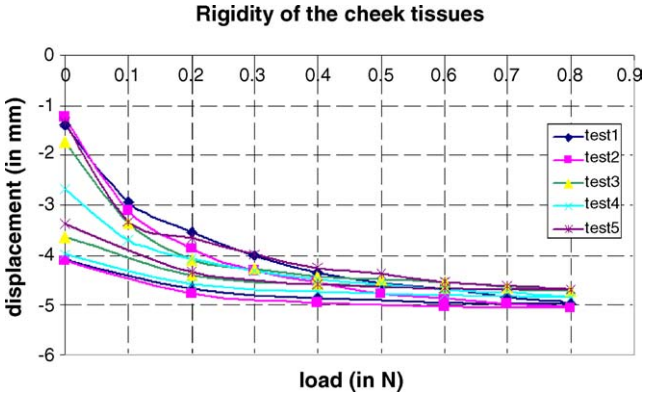

Fig. 2. Results of indentation (forward and backward path) for cheek tissues directly measured from indenting device.

case, respectively, in pressure or in traction. The advantage of such actuators is to guarantee a great accuracy either in load or in displacement. Indeed, Enduratec gives the possibility to monitor the load with 0.02 N steps or the displacement with 1 μm steps. Nevertheless, this device is not able to apply load larger than 225 N and displacement exceeding 13 mm. It is therefore well adapted to the study of soft tissue properties, since their rigidity is relatively low.

For this experiment, the tongue and a piece of the cheek were removed from the fresh cadaver of a 74 year old woman. The indentation experiment was run less than 24 h after death, in order to limit tissue deterioration. Tongue was indented at ambient temperature, a little less than normal human body temperature. This temperature gap was assumed not to affect mechanical tissues properties, assuming that their thermal dilatation coefficients are low. The Enduratec jaws have been used to hold a 14 mm radius cylinder, in order to apply a vertical load on the tongue or cheek tissues. The load case applied on the soft tissues consisted in a linear ramp composed of single steps. Between two successive steps, a load increase of 0.1 N was achieved. A few seconds break had to be observed after each step to allow the tissues to effectively reach the measured equilibrium displacement of the 0.1 N step. Loads were applied from 0.1 to 0.8 N, the maximum load being chosen in order not to deteriorate the fibre structures. The displacement measured at each step and the corresponding load are plotted to get the curve showing the displacement as a function of the load. It gives an estimation of the tissues stiffness.

Fig. 2 plots results from five round load cases (progressive loading and unloading) measured with a pressure exerted on the middle of the same cheek specimen. The results point out that the relationship between the load imposed to the tissues and the resulting displacement is non-linear. For each condition the upper part of the curve corresponds to the compression from load 0 N to load 0.8 N, while the lower part draws the behavior during the release.

As a first observation, one can notice the high variability of these indentation results provided for the cheek specimen. A clear hysteresis effect is observed, probably due to the crushing of the soft tissues during the loading. The high complexity of facial tissues, made of uneven layers of skin, fat and muscle, can also explain the variability.

Because of this observed variability and because tongue modeling is the main focus of our speech production study, it was decided to carry out the tongue indentation experiment with more specificities. Tongue being covered with a layer of mucosa, it was chosen to measure separately the mechanical properties of the mucosa and those of the tongue body, mainly composed of muscles. Indeed, the mucosa that can surround anatomical structures is often known as having different stiffness than the inner part of the structure (see, for example, the liver, where the stiffness of the Glisson capsule is higher than the one of the parenchyma tissues [18]). Two types of indentations were therefore successively carried out: the first was applied to the whole tongue (including the mucosa); for the second one, the mucosa layer was removed and the remaining part was indented. In each case, the indentation was made at the rear and at the front of the tongue, in order to test the possible limits of the assumption of isotropy that was primarily chosen in the first version of our 3D tongue model [10]. In summary, four different indentation experiments were made: (1) front of the tongue, with mucosa; (2) front of the tongue, without mucosa; (3) rear of the tongue, with mucosa; (4) rear of the tongue, without mucosa. For each experiment, five round load cases (progressive loading and unloading) were carried out. Fig. 3 plots the results obtained for the four experiments. Here again, we can notice the non-linear mechanical behavior of the tissues.

4. A constitutive law for the tongue tissues: finite element analysis

The indentation experiment itself does not provide the constitutive law of the material. Indeed, the measurements only give the relationship between the local force applied to the external surface of the body and the resulting displacement. To get the constitutive law from this indentation experiment, i.e. the global relationship that can be assumed between strain and stress inside the body, an optimization algorithm based on an "*analysis by synthesis*" strategy was elaborated. It consisted in (1) assuming a given constitutive law, (2) building a finite element analysis (FEA) of the indentation experiment, (3) comparing the simulations provided by this FEA with the indentation measurements, (4) using this comparison to propose a change of the constitutive law that should make the FEA simulations and the measurements closer, and (5) starting again with (2) up to the point where the comparison carried out in (3) gives satisfactory results.

4.1. Choice for a constitutive law

According to Fung [15], a hyperelastic material seems to be well adapted for human soft tissues. A material is said to be hyperelastic if it is possible to find a function W, called the

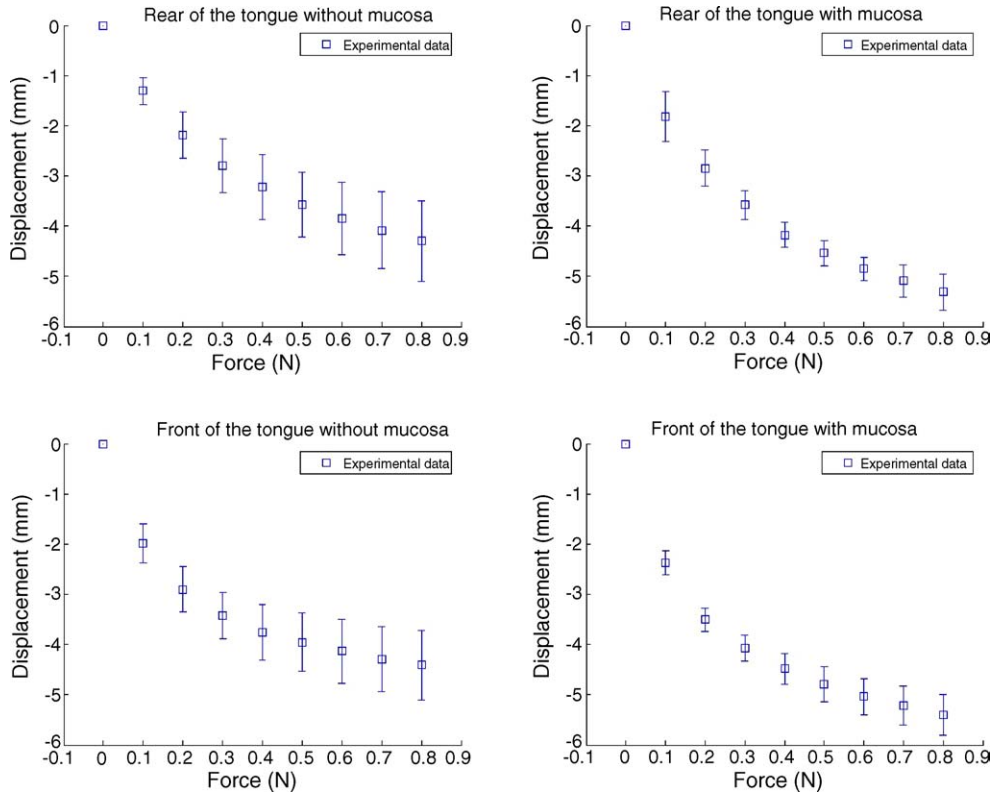

Fig. 3. Results of indentation for the front (bottom panels) and rear (top panels) parts of the tongue, with (right panels) and without mucosa (left panels); squares represent the average values of the measures for each force level; vertical bars indicate the corresponding standard deviation.

strain-energy function, the derivative of which with respect to the strain tensor ε equals the stress tensor σ. Among the various strain-energy functions which can describe such a mechanical response [21], we focused on the incompressible two parameter Yeoh strain-energy function W, already used to characterize tissues and living cells [22,23]. This strain-energy function is given by the following analytical expression [21]:

$$W = a_{10}(I_1 - 3) + a_{20}(I_1 - 3)^2 \quad (1)$$

where a_{10} and a_{20} are the two material constants (having a unit of stress), while I_1 is the first invariant of the right Cauchy–Green strain tensor C ($I_1 = \mathrm{Trace}(C)$). From this strain-energy W, it is therefore possible to compute the stress/strain relationship, i.e. the material constitutive law.

4.2. Finite element analysis of the indentation experiment

Computations of the cylindrical indenter displacement induced by increasing value of the applied force were performed using a finite element (FE) approach (ANSYS 5.7 software, ANSYS Inc., Cannonsburg, PA, USA). The FE method is a computerized technique dividing a complex structure into small sections (elements) so that simpler functions may be used to derive the strain and stress distributions.

A refinement of the present numerical analysis consisted in taking into account the progressive increase in contact area between the indenter and the tissue medium as the indenter displacement increases. We meshed with specific elements two potential contact surfaces, thanks to the "rigid-to-flexible" elements provided in ANSYS software. The indenter surface was treated as rigid, since it had actually a much higher stiffness than the deformable tissues. The contact algorithm selected to solve our problem is the Augmented Lagrangian method. This method computes the additional nodal forces that avoid the penetration of the solid indenter in the soft tissue elements. Due to the symmetry of revolution of the mechanical properties of lingual tissues, of the indenter, of the specimen geometries, and of boundary conditions, the computations were performed on a quarter of the specimen. The following displacement conditions were imposed on the tissue boundaries: (i) zero displacement, modeling full attachment to the basal plane, was imposed to the lingual tissues in contact with the base; (ii) zero stress conditions were assumed for the external upper free surface; (iii) zero normal displacement conditions were imposed on the sections belonging to the planes of symmetry; (iv) free boundary conditions for the lateral surfaces.

In order to derive the mechanical properties of the mucosa and of the inner tongue tissues from the experiments described below, two numerical analyses were performed: the first simulated the indentation of the inner tissues alone,

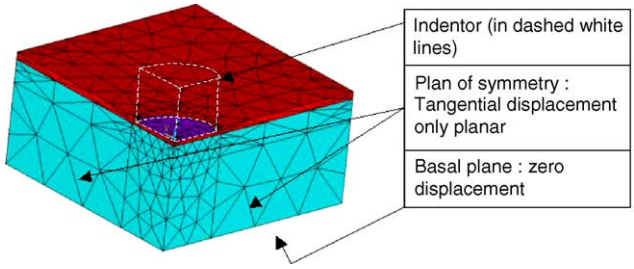

Fig. 4. Mesh used for numerical simulation of the indentation. Free boundary conditions are considered, except when explicitly indicated on the figure.

while the second considered the bi-layer structure including the mucosa. Fig. 4 presents the FE mesh (a quarter of the specimen of tongue with mucosa) that was used for the simulation of the indentation experiment. One can see, at the top of the mesh, the thin layer of elements that models the mucosa.

4.3. Constitutive law: fitting the FE simulations with the indentation measurements

An iterative algorithm (integrated in the ANSYS software) was defined to compute a_{10} and a_{20} values that confer to the FE material a mechanical behavior close to the one described by the indentation measurements. It was not possible to compute the two coefficients a_{10} and a_{20} in a serial way, as they are not totally independent from each other. Knowing that a_{10} mainly influences the linear part of the constitutive law (corresponding to small deformations), the first measurement point (the 0.1 N load) was used to iteratively infer the a_{10}. Similarly, the last measurement point (the 0.8 N load) was used to infer the initial a_{20} value. Our guess was that finding a_{10} and a_{20} values by only fitting the two extreme points (0.1 and 0.8 N points) would be sufficient to get a global fitting of the curves, which is satisfactory for the whole domain of variation of the load.

Let n be the step number of the iterative algorithm, a_{10_n} and a_{20_n} the strain-energy parameters and u_{1_n} and u_{8_n} the FE simulated displacements respectively for a 0.1 N and a 0.8 N load. Let U_1 and U_8 be the target displacements measured during the indentation experiment, respectively for a 0.1 N and a 0.8 N load. As we assume that a_{10} linearly determines the displacement for small loads, a_{10_n+1} at iteration $n+1$ can be computed as:

$$a_{10\_n+1} = a_{10\_n}\frac{u_{1\_n}}{U_1} \tag{2}$$

The computation of a_{20_n+1} is made as follows. If $|u_{8\_n}| > |U_8|$, i.e. if the simulated displacement is larger than the measured one, it means that, in the non-linear part, the material is not stiff enough, and a_{20_n} has to be increased. On the contrary, if $|u_{8\_n}| < |U_8|$, a_{20_n} has to be decreased. Two convergence criteria, α and β, were defined, respectively for u_{1_n} and u_{8_n}. In a first step, the value of a_{10} is optimized until $|u_{1\_n} - U_1| < \alpha$; then, in a second step, the value of a_{20} is updated one time. As the change of value of

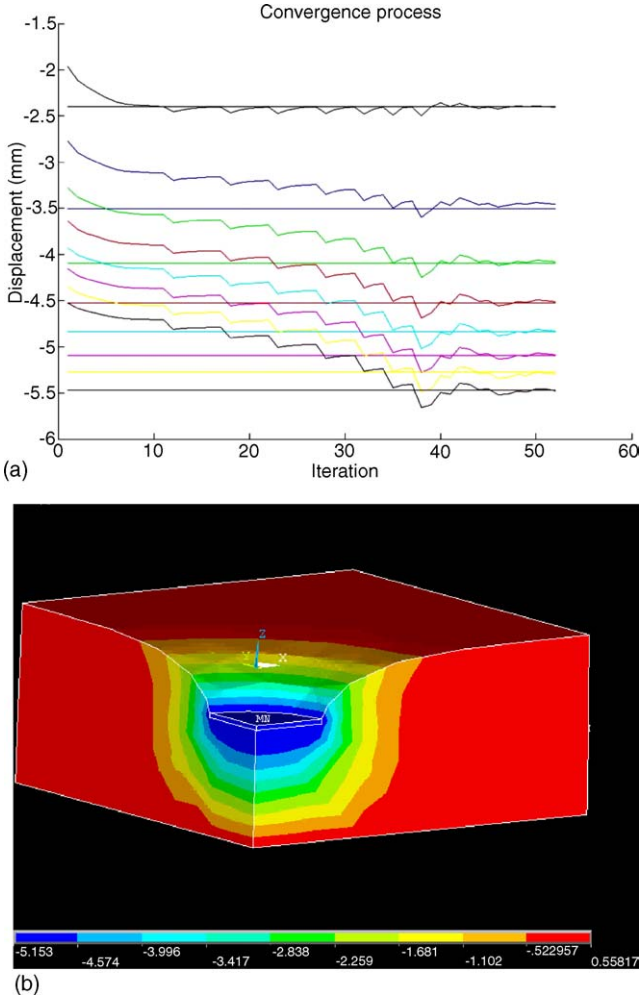

Fig. 5. Top: convergence curves for each measurement point. Bottom: example of the deformation of the FE structure in the simulated indentation.

a_{20} will modify the simulated displacement for 0.1 N, another optimization of a_{10} is made. The whole process is repeated until both convergence criteria are reached: $|u_{1\_n} - U_1| < \alpha$ and $|u_{8\_n} - U_8| < \beta$. Under this condition, we obtained for the eight simulated displacements a maximum relative error of 1.5%, representing a maximum of 80 μm absolute error on displacement. At this iteration ($n = 50$) it was considered that the optimal parameter values were reached and that $a_{10} = a_{10\_n}$ and $a_{20} = a_{20\_n}$.

Fig. 5 (top panel) plots the convergence curves provided by the iterative fitting algorithm toward each of the eight measured displacements (for the rear of the tongue and without mucosa). As can be seen, each of the eight targets is very well approximated within fifty iterations. The bottom panel of Fig. 5 plots the finite element simulations of the indentation experiment provided with the corresponding constitutive law.

Fig. 6 superposes the constitutive laws derived from the optimization process with each of the four indentation experiments measurements. As can be seen, the non-linear laws extracted from the optimization algorithm are consistent with

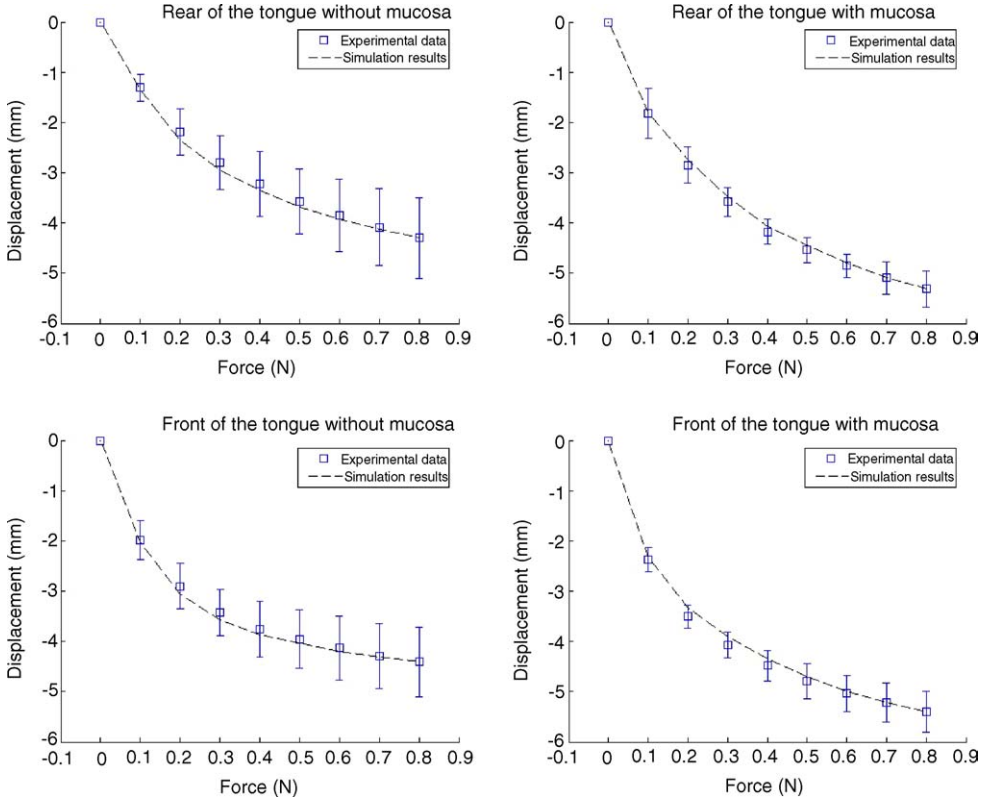

Fig. 6. Force/displacements curves obtained with the optimal constitutive laws (dashed line) with mucosa (right panels) and without mucosa (left panels); the results of the indentation experiment are superimposed (see Fig. 3 for details).

Table 1
Results of the iterative algorithm: a_{10} and a_{20} values obtained for each of the four tongue indentation experiments

	a_{10} value (Pa)	a_{20} value (Pa)
Front part of the tongue	190	87
Rear part of the tongue	199	89
Rear part of the tongue without mucosa	193	92
Front part of the tongue without mucosa	184	95
Mean value	191.5	90.6
Standard deviation	6.2	3.5

the data provided by the measurements. Table 1 summarizes the a_{10} and a_{20} values thus obtained for each of the four different conditions.

Given the accuracy of the measurement, it can be considered that the differences between the parameter values inferred with and without mucosa are not significant. As a consequence, a single constitutive law was adopted for the whole tongue body ($a_{10} = 191.5$ and $a_{20} = 90.6$), without adding a specific layer of elements to simulate the mechanics of the mucosa.

5. A 3D finite element model of the human tongue

The constitutive law thus inferred from the indentation experiments was used in the 3D biomechanical model that we are currently developing. The model consists of a 3D finite element mesh (Fig. 7) that was designed on the basis of anatomical data extracted from the Visible Human Project®'s female data set, and of morphological studies of tongue musculature. The design procedure of this mesh is described in details in [10]. Tongue muscle arrangement within the FE mesh is modeled by individual sets of adjacent elements. In addition, a main fibres direction was defined for each muscle within the associated set of elements. In order to facilitate further quantitative comparisons of simulations with experimental data collected on real speakers, the external geometry of the initial mesh was matched to the 3D tongue shape of a human speaker, while preserving the internal structure. Reference data on the speaker consisted in the association of MRI images, CT scans (for bony structures like jaw and hyoid bone), and a plaster cast of the palate optically scanned to digitize the information.

The model was tested with force levels compatible with speech movements. Muscle activations were functionally modeled by an external generator that applies forces on the nodes of each set of elements. The generated forces are oriented along the main fibres direction and they are mostly concentrated at the two muscle extremities in this direction (see [1] for more details about this functional muscle model). The duration of each simulation is 120 ms and the forces are applied as a step function for all simulations. The general behavior of the model is satisfactory, since very realistic

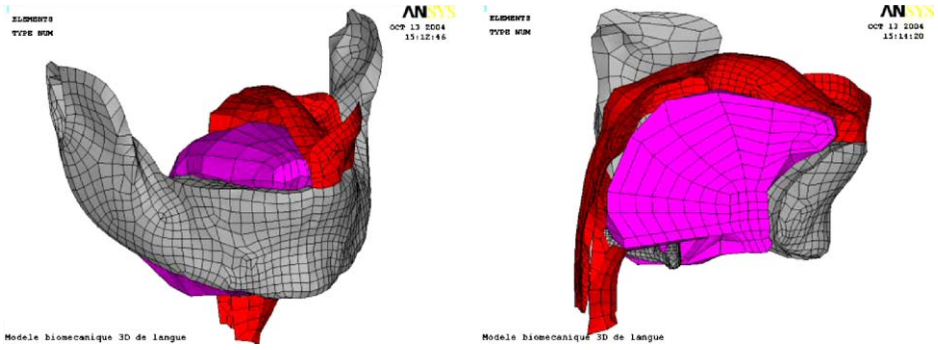

Fig. 7. Side and sagittal views of the 3D finite element mesh.

tongue deformations have been obtained with realistic level of forces and within realistic durations [10,24]. In order to illustrate that simulations obtained with the model can help understanding how the central nervous system controls the tongue during speech production, two examples of results are presented.

The first simulation was achieved with a 2 N force generated by the posterior genioglossus (GGp) and a 0.2 N force generated by the anterior genioglossus (GGa). The resulting tongue shape is shown on Fig. 8. The posterior genioglossus is known [25] to be the main muscle involved in the production of vowel [i]. The vocal tract geometry classically observed for this vowel corresponds to a front articulation, with a large pharyngeal cavity and a constriction in the alveopalatal region. In addition, in the constriction region and still for [i], the tongue shape in the coronal plane is characterized by a grooving, the central part of the tongue being lower than the sides. Former simulations with the model of the impact of GGP on the tongue shape did generate the expected front articulation, but no grooving of the tongue could be observed [24]. On the other hand, simulations of the impact of the GGa did show a grooving of the tongue together with a lowering and a backward displacement of the tongue. For this reason, in order to properly simulate the articulation of vowel [i], we tested the impact of both muscles simultaneously with a larger activation of the GGp, in order to reach the front articulation and the grooving. Fig. 8 shows that under these conditions, the tongue is pushed forward and high in the alveolar region, and that a grooving exists in the front part of the tongue. This simulation demonstrates thus that the grooving of the tongue for [i] is not the result of the only activation of the GGp, but rather the consequence of the combined activation of GGp and GGa.

The second simulation was obtained with a 0.5 N force generated by the superior longitudinalis (SL). This muscle known to be activated during the production of alveolar stops such as [t] where the tongue tip is in contact with the palate in the alveolar region. The final tongue shape is depicted on Fig. 9. As expected a clear elevation of the tongue tip can be observed. However, it can also be observed that the tongue

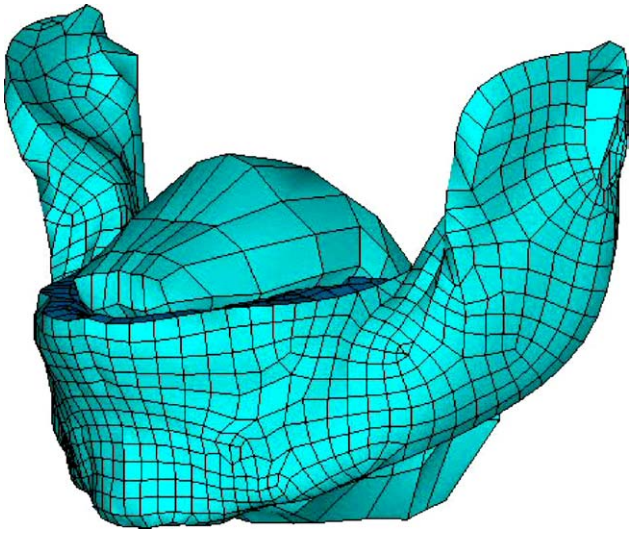

Fig. 8. 3D view of the final tongue shape reached with a 2 N and a 0.5 N force produced respectively by the GGp and the GGa (see text for details).

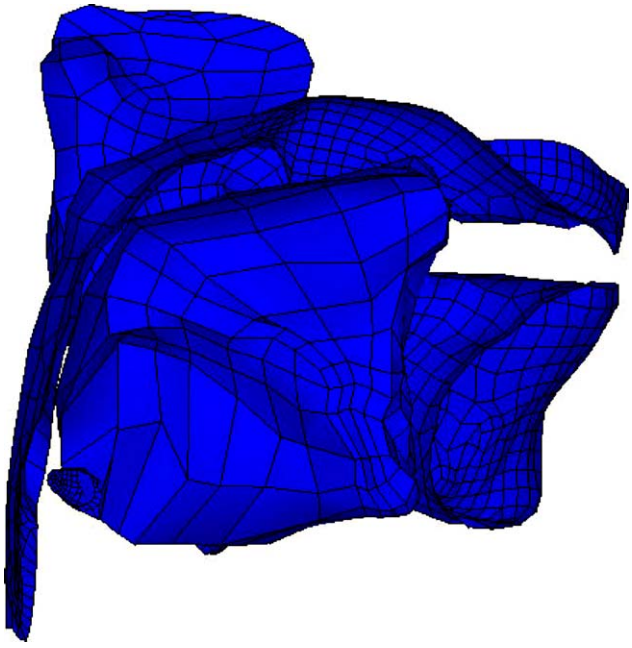

Fig. 9. 3D view (from the left hand side) of the final tongue shape reached with a 0.5 N force produced by the superior longitudinalis.

dorsum is high in the velar region, which is not compatible with data on the production of [t] in all vowel contexts except with [i]. It can be concluded that the production of [t] necessitates not only the activation of SL, but also the activation of other muscles that will flatten the tongue in the velar region, such as the middle part of the Genioglossus, GGm.

6. Conclusion and prospects

In order to use physical models of the speech production apparatus to test hypotheses about speech motor control and to understand how speech perception could make use of knowledge about the physical properties of speech articulators, we have to rely on a realistic account of these properties. In this paper, we have presented an experimental approach based on an indentation procedure to characterize how tongue and facial tissues deform when forces in the muscle force magnitude are applied to them. We have shown that hyperelastic non-linear functions allow a good account of the data, even if this study is a very preliminary one with some limitations: (1) an isotropic and homogeneous behavior of the tissues is assumed whereas the mechanical complexity of lingual and facial tissues is well known (interwoven muscle fibers, layers of skin, fat); (2) a unique specimen of tongue and cheek tissues was indented whereas it is known that the rheology of soft tissues is highly variable from one person to another one. However, we believe our findings are of particular interest, especially in the case of lingual tissues, since there is no data in the literature about tongue tissues, in spite of the fact that it is a major articulator to produce speech, which is the basis of human communication.

The 3D tongue model using the thus inferred constitutive law has been proved to behave in a realistic way even if its FE mesh is pretty coarse (mainly because the computation times required to simulate a speech movement are important); we should therefore study more precisely the way the mesh density affects the accuracy of the results. By comparing its simulations with kinematic data collected onto a real speaker, the model will become a promising tool to test hypotheses about speech motor control. It should also be used for pathological applications as a tool to help surgeons planning medical gestures during glossectomy or sleep apnea surgery. In both cases, this model could be used to estimate the impact of surgery gestures on patient's speaking abilities, and if necessary help surgeons to plan a different surgery strategy, less disturbing in terms of speech production abilities.

Acknowledgements

The authors are very indebted to Professor Jacques Lebeau, from Grenoble University Hospital (France), who provided them with the fresh cadaver tongue, and to Professor Pascal Swider, from the Toulouse Biomechanics Lab (France), for providing the Enduratec device. The European Cooperative Research Project DISHEART (Grid based decision support system for assisting clinical diagnosis and interventions in cardiovascular problems) is also acknowledged for its financial support.

References

[1] Payan Y, Perrier P. Synthesis of V–V sequences with a 2D biomechanical tongue model controlled by the equilibrium point hypothesis. Speech Commun 1997;22(2/3):185–205.
[2] Perrier P, Payan Y, Zandipour M, Perkell J. Influences of tongue biomechanics on speech movements during the production of velar stop consonants: a modeling study. J Acoust Soc Am 2003;114(3): 1582–99.
[3] Perkell JS, Klatt D, editors. Invariance and variability of speech processes. Hillsdale, NJ: Lawrence Erlbaum Assoc; 1986.
[4] Viviani P, Stucchi N. The effect of movement velocity on form perception: geometric illusions in dynamic displays. Percept Psychophys 1989;46:266–74.
[5] Munhall KG, Servos P, Santi A, Goodale MA. Dynamic visual speech perception in a patient with visual form agnosia. Cogn Neurosci Neuropsychol Neuroreport 2002;13(14):1793–6.
[6] Gomi H, Kawato M. Equilibrium-point control hypothesis examined by measured arm stiffness during multijoint movement. Science 1996;272:117–20.
[7] Gribble PL, Ostry DJ, Sanguineti V, Laboissière R. Are complex control signals required for human arm movement? J Neurophysiol 1998;79:1409–24.
[8] Perrier P. About speech motor control complexity. In: Harrington J, Tabain M, editors. Speech production: models, phonetic processes, and techniques. Sydney, Australia: Psychology Press, in press.
[9] Laboissière R, Ostry DJ, Feldman AG. Control of multi-muscle systems: human jaw and hyoid movements. Biol Cybernet 1996;74:373–84.
[10] Gerard JM, Wilhelms-Tricarico R, Perrier P, Payan Y. A 3D dynamical biomechanical tongue model to study speech motor control. Recent Res Develop Biomech 2003;1:49–64.
[11] Chabanas M, Luboz V, Payan Y. Patient specific finite element model of the face soft tissue for computer-assisted maxillofacial surgery. Med Image Anal 2003;7(2):131–51.
[12] Perrier P, Payan Y, Marret R. Modéliser le physique pour comprendre le contrôle: le cas de l'anticipation en production de parole. In: Sock R, Vaxelaire B, editors. L'Anticipation à l'horizon du présent. Sprimont, Belgique: Pierre Margala Editeur; 2004. p. 159–77.
[13] Bonet J, Wood RD. Non-linear continuum mechanics for finite element analysis. Cambridge University Press; 1997.
[14] Napadow VJ, Chen Q, Wedeen VJ, Gilgert RJ. Intramural mechanics of the human tongue in association with physiological deformations. J Biomech 1999;32:1–12.
[15] Fung YC. Biomechanics: mechanical properties of living tissues. New York: Springer-Verlag; 1993.
[16] Del Prete Z, Antoniucci S, Hoffman AH, Grigg P. Viscoelastic properties of skin in Mov-13 and Tsk mice. J Biomech 2004;37: 1491,1497.
[17] Miller K, Chinzei K. Mechanical properties of brain tissue in tension. J Biomech 2002;35(4):483–90.
[18] Carter FJ, Franck TG, Davies PJ, Cuschieri A. Puncture forces on solid organ surfaces. Surg Endoscopy 2000;14:783–6.
[19] Schmidlin FR, Schmid P, Kurtyka T. Force transmission and stress distribution in a computer simulated model of the kidney: an analysis of the injury mechanisms in renal trauma. J Trauma 1996;40:791–6.
[20] Lin DHS, Yin FCP. A multiaxial constitutive law for mammalian left ventricular myocardium in steady-state barium contracture or tetanus. J Biomech Eng 1998;120:504–17.

[21] Holzapfel GA. Non-linear solid mechanics. Chichester: Wiley & Sons; 2001. p. 455.
[22] Ohayon J, Tracqui P, Fodil R, Laurent VM, Planus E, Isabey D. Finite element analysis of strain hardening properties of adherent epithelial cells assessed by magnetic bead twisting. J Biomech Eng 2004;126:685–98.
[23] Costa KD, Yin FCP. A nalysis of indentation: implications for measuring mechanical properties with atomiv force microscopy. J Biomech Eng 1999;121:462–70.
[24] Gerard JM, Perrier P, Payan Y. 3D biomechanical tongue modeling to study speech production. In: Harrington J, Tabain M, editors. Speech production: models, phonetic processes, and techniques. Sydney, Australia: Psychology Press, in press.
[25] Baer T, Alfonso PJ, Honda K. Electromyography of the tongue muscles during vowels in/↔pVp/environment. Annual Bulletin, Research Institute of Logopedics and Phoniatrics, Tokyo University, 1998:7–19.